ELSEVIER

Polymer Vol. 37 No. 2, pp. 313–319, 1996
Copyright © 1996 Elsevier Science Ltd
Printed in Great Britain. All rights reserved
0032-3861/96/$15.00+0.00

Characterization of branched polyethyleneimine by laser light scattering and viscometry

Il Hyun Park* and E-Joon Choi
Department of Polymer Science and Engineering, Kumoh National University of Technology, Kumi, Kyungbuk, 730-701, Korea
(Received 30 March 1995)

A series of seven fractions of branched polyethyleneimine (BPEI) spanning a molecular weight range 1.7×10^4–5.3×10^6 g mol^{-1} were characterized by means of laser light scattering and viscometry at 35°C. The weight-average molecular weight, M_w, the second virial coefficient, A_2^*, the z-average radius of gyration, R_G, the z-average effective hydrodynamic radius, R_H, the intrinsic viscosity, $[\eta]$, and the Huggins coefficient, K_H, were determined in 1 M NaCl aqueous mixture solvent. Based upon these experimental results, the scaling relations between M_w and the various kinds of radii were established. The exponents of the relations appeared to be much smaller than the generally accepted value for a linear polymer chain (for example, the Mark–Houwink equation; $[\eta] = 0.513 M_w^{0.31}$). Also some ratios such as R_G/R_H and R_G/R_T showed a molecular weight dependence, where R_T $[= (3A_2^* M_w^2/16\pi N_A)^{1/3}]$ was defined as the thermodynamic radius. Although quantitative comparison with theories was somewhat restricted due to the slightly high index of polydispersity ($M_w/M_n = 1.8$–2.2) of the BPEI fractions, it was found that the structure of BPEI seemed to be randomly branched and became more compact with increasing molecular weight.

(Keywords: branched polyethyleneimine; light scattering; solution properties)

INTRODUCTION

Numerous experimental studies of the space-filling properties of branched polymers in dilute solution have been conducted over the last few decades[1–15]. Most of these studies have involved model polymers such as polystyrene[2–4], polyethylene[5–9], polyvinylacetate[10–12] and polyisoprene[13]. In contrast, rigorous studies concerning the dilute solution properties of branched polyethyleneimine (BPEI) are rarely found[16,17]. This might be because, unlike the model polymer chain, BPEI has not only short rather than long branches but also a weak polyelectrolyte character[18]. From the experimental point of view, such structure and character make both fractionation for the narrow molecular weight distribution and application of theories difficult. In this work, we used an extraction fractionation technique which was developed by Van Den Berg *et al.*[16]. The thermodynamic and hydrodynamic properties of BPEI polymers in 1 M NaCl aqueous mixture solvent were investigated by means of static and dynamic light scattering, and viscometry. The results were compared with previously reported experimental data as well as with theoretical values. Through parameters such as the exponents of the scaling relations and the size ratios of two different kinds of radii, we examined how the branching effect is introduced into the structure of BPEI with increasing molecular weight.

* To whom correspondence should be addressed

EXPERIMENTAL

Materials

The two branched polyethyleneimine (BPEI) samples used in this study were purchased from Polyscience (BPEI(A): catalogue no. 19850, nominal $M_w = 10\,000$ g mol^{-1}, 100% liquid state; BPEI(B): catalogue no. 00618, nominal $M_w = 70\,000$ g mol^{-1}, aqueous solution state). The exact content of water (32.1 wt%) in the BPEI(B) sample was quantitatively determined by reweighing the sample after complete evaporation of water in a vacuum oven at 60°C overnight.

Fractionation

Under the assumption that the higher molecular weight branched polymer fraction had more branching points, the BPEI(B) sample of higher molecular weight was fractionated by the extraction fractionation method. It utilized the difference of solubility between HCl-coordinated BPEI and acid-free BPEI. Van Den Berg *et al.*[16] reported that this fractionation method was more efficient than the conventional precipitation fractionation in obtaining fractions of narrow molecular weight distribution (*MWD*). The details of this fractionation were as follows. The BPEI/water solution with a concentration of ~5 wt% was acidified with HCl to pH ~1.5. Sufficient ethanol was added to make the solution milky. The milky solution was allowed to stand at room temperature for phase-separation into two clear layers. The BPEI polymers in the upper layer were bound by smaller numbers of HCl molecules than those in the

lower layer. Extraction of the upper layer was followed by acidifying it with HCl up to pH ~1.0. Excess ethanol was again added into this solution to precipitate almost all BPEI polymers of the upper layer. Since the fractionated BPEI polymers were coordinated with HCl, they were treated with a strong OH^- ion-exchange resin (Sigma Amberlite IRA-400 OH) overnight to give HCl-free BPEI polymers. This acid-free fraction still included a small amount of ethanol and fine particles of resin. These optical impurities were filtered with a 0.45 μm membrane filter and all volatile solvents were removed by a rotary evaporator. This fraction was redissolved into freshly distilled water, its concentration was determined by means of a differential refractometer (see below) and it was then stored in a desiccator to prevent contamination by carbonate ions from the air. Subsequently, the lower layer was diluted 20–30 times by volume with pure water and then acidified again with HCl to pH ~1.5. The same procedures were repeated to obtain another fraction of the BPEI sample. As a result, nine fractions were obtained but only seven fractions in the range of $M_w/M_n = 1.8$–2.2 were analysed in this study so that at least the same amount of polydispersity effect was given to each fraction. Generally, the branched chains of each fraction may have different branching frequencies and branched lengths even after fractionation. Therefore, our BPEI fractions do not represent well defined polymer fractions of uniform branching frequencies and lengths.

dn/dC and determination of concentration

The values of dn/dC of BPEI in various solvents were measured using a home-made differential refractometer at $\lambda_0 = 632.8$ nm and 35°C: BPEI/H_2O, 0.210 ml g^{-1}; BPEI/1 M NaCl aqueous solution, 0.195 ml g^{-1}; BPEI/methanol, 0.225 ml g^{-1}. Van Den Berg *et al.*[16] reported that in BPEI/H_2O, $dn/dC = 0.216$ ml g^{-1} at $\lambda_0 = 589.3$ nm and 25°C. The concentration of the fractionated BPEI mother solution was easily determined by measuring the difference between the refractive index of the mother solution and that of pure water.

Viscosity

Viscosity of the polymer solution, η, was measured using a Ubbelohde viscometer at 35°C. Precision in the flow times was 0.05 s, and the temperature of the water bath was controlled to ±0.02°C. Kinetic energy correction was negligible in the calculation of viscosity due to the long flow time (> 180 s). Intrinsic viscosity, $[\eta]$ was determined by means of Huggins (η_{sp}/C *versus* C) and Kraemer ($\ln \eta_r/C$ *versus* C) extrapolations, where η_{sp} ($= \eta/\eta_0 - 1$) is the specific viscosity and η_r ($= \eta/\eta_0$) the relative viscosity, respectively.

Static light scattering

A commercial laser light-scattering spectrometer (Brookhaven BI-200SM detector system, BI-9000AT digital correlator) was used with a He–Ne laser (Spectra Physics model 127, operated at $\lambda_0 = 632.8$ nm and 35 mW). Both the incident beam and the scattered beam were vertically polarized. The scattered intensity was calibrated with benzene and the weight-average molecular weight, M_w, and the z-average radius of gyration, R_G, were obtained by means of a Zimm plot:

$$\frac{HC}{R_{VV}} = \frac{1}{M_w^*}(1 + q^2 R_G^2/3) + 2A_2^* C \qquad (1)$$

where $H = 4\pi^2 n^2 (dn/dC)^2 / N_A \lambda_0^4$ is an optical constant, R_{vv} is the excess Rayleigh ratio for the vv component, and $q = (4\pi n/\lambda_0)\sin(\theta/2)$ is the magnitude of the scattering vector. Light scattering measurements under the mixture solvent (i.e. 1 M NaCl aqueous solution) lead to the apparent molecular weight, M_w^*, and the second virial coefficient, A_2^*. The relations between these quantities and those of M_w and A_2 in the pure water system may be written as[19]:

$$M_w^* = M_w(1 + \gamma)^2 \qquad (2)$$

$$A_2^* = A_2 \Gamma(M, Z, C_s, \alpha) \qquad (3)$$

where the coefficient γ comes simply from the preferential adsorption effect but the coefficient Γ is a complex function of the molecular weight of the polyelectrolyte M, the number of charges on the single polymer chain Z, the salt concentration C_s, and the expansion factor of the chain α[19].

Dynamic light scattering and polydispersity index

The time autocorrelation function (TAF) of the scattered intensity $G^{(2)}(t)$ has the form:

$$G^{(2)}(t) = A(1 + b|g^{(1)}(t)|) \qquad (4)$$

where A is the background, b is the optical beating efficiency and $g^{(1)}(t)$ is the normalized correlation function of the scattered electric field. For polydisperse polymers in solution, $|g^{(1)}(t)|$ is given as

$$|g^{(1)}(t)| = \int G(\Gamma)\exp(-\Gamma t)\, d\Gamma$$

(for a polydisperse sample) (5)

where $G(\Gamma)$ is the normalized characteristic linewidth distribution. The z-average characteristic linewidth, $\langle\Gamma\rangle$ and the variance could then be determined by the second-order cumulant method. The effective hydrodynamic radius, R_H, of the polymer chain was calculated from the z-average translational diffusion constant, D_0, by means of the Stoke–Einstein equation:

$$D_0 = (\langle\Gamma\rangle/q^2)_{C=0,\theta=0} = k_B T/6\pi\eta_0 R_H \qquad (6)$$

where k_B is the Boltzmann constant and T is the absolute temperature, respectively. The polydispersity index M_w/M_n of each fraction was computed from the molecular weight distribution (*MWD*), which was transformed from the characteristic linewidth distribution $G(\Gamma)$ using the scaling relation between the translational diffusion constant and molecular weight[20]. In order to minimize the correction factors such as concentration dependence and the effect of internal motion, the time autocorrelation function (TAF) was measured at low concentration and low scattering angle of $qR_G < 1$. The CONTIN program was also used for calculation of $G(\Gamma)$ from TAF. Although we used the scaling relation obtained from polydisperse fractions rather than monodisperse ones, it was found that M_w/M_n was not affected by the scaling constant, which controlled only parallel movement of the *MWD* in the logarithmic molecular weight space of the x-axis. For the

M_w/M_n value approximated by this method, the relative error was about 10%.

Viscometric radius and thermodynamic radius

The viscometric radius, R_V[21], and thermodynamic radius, R_T[22], are calculated from the intrinsic viscosity and the second virial coefficient using equations (7) and (8), respectively:

$$R_V = (3M_w[\eta]/10\pi N_A)^{1/3} \quad (7)$$

$$R_T = (3A_2M_w^2/16\pi N_A)^{1/3} \quad (8)$$

RESULTS AND DISCUSSION

Polyelectrolyte character and salt effect

The intrinsic viscosity of unfractionated BPEI(B), 32.0 ml g^{-1}, in pure water, decreases to 23.0 ml g^{-1} in 1 M NaCl aqueous solution. This result indicates that the BPEI polymer is intrinsically a weak polyelectrolyte. To find how much the polyelectrolyte character affects the solution properties of the fractions obtained from this particular fractionation, we measured the inherent viscosity of the F6 fraction as a function of the NaCl concentration. As shown in *Figure 1*, the polyelectrolyte effect is more pronounced in the fraction than in the original BPEI. We can attribute this behaviour to the residual HCl molecules bound at the tertiary N atoms of the fractionated BPEI chain. The residual amount of HCl was estimated as an order of ~0.2 mol% by analysing its turbidity after titration of the fractionated mother solution with $AgNO_3$ solution. As the polyelectrolyte behaviour renders the analysis of the branching effect difficult and also is not the subject of this study, we in fact added excess NaCl salt (say, 1 M NaCl) to all polymer solutions both for the light-scattering experiment and for viscosity measurements to eliminate this effect.

Light scattering

Since the values of dn/dC listed in the Experimental section are determined at constant solvent composition rather than at constant chemical potential of the solvents, the molecular weight obtained becomes the apparent value due to the effect of preferential adsorption. For the

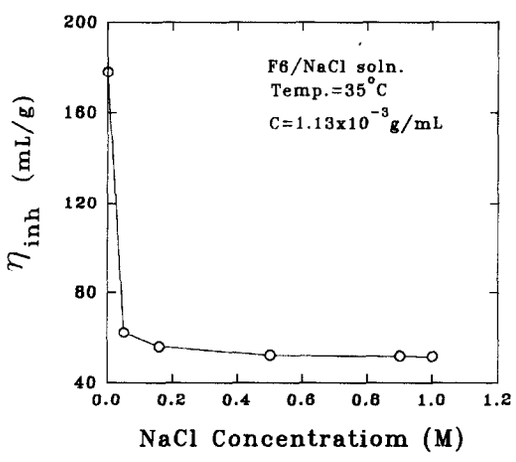

Figure 1 A plot of inherent viscosity against the added NaCl concentration in the F6 fraction. The polyelectrolyte effect was efficiently suppressed at 1 M NaCl

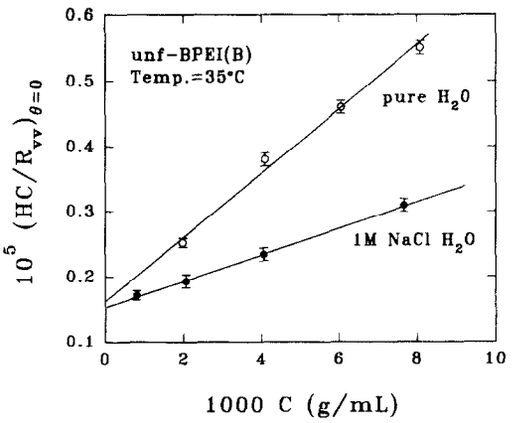

Figure 2 Variation of $(HC/R_{vv})_{\theta=0}$ against concentration of unfractionated BPEI(B) in two different solvent systems. The true weight-average molecular weight is obtained from the apparent molecular weight measured in 1 M NaCl aqueous mixture solvent by multiplying by a factor of 0.925

estimation of this effect, the Rayleigh ratios of the unfractionated BPEI(B) sample are measured both in pure water and in 1 M NaCl mixture solvent, and are plotted as a function of concentration in *Figure 2*. From the intercepts of the y-axis in *Figure 2*, we obtain the following results: the apparent molecular weight, $M_w^* = 6.55 \times 10^5$ g mol^{-1} in 1 M NaCl mixture solvent, the true molecular weight, $M_w = 6.06 \times 10^5$ g mol^{-1} in pure water (it should be noted that the manufacturer's nominal M_w of 7×10^4 g mol^{-1} is lower than the true M_w by nearly one order of magnitude). Hereafter, the true molecular weight has always been calculated by multiplying the factor of 0.925 ($= 6.06 \times 10^5/6.55 \times 10^5$) by the apparent molecular weight obtained in the 1 M NaCl mixture solvent.

If only the preferential adsorption effect appears in this mixture solvent system, the Γ ratio ($\equiv A_2^*/A_2$) in equation (3) can be simplified[19] as $1/(1+\gamma)^2$ and in this particular case its value is about 1.08 ($= 1/0.925$). As shown in *Figure 2*, however, the A_2 value in a single solvent is much larger, by a factor of 2.38, than the A_2^* measured in a mixed solvent. It is certain that NaCl provides not only the preferential adsorption effect but also the screening effect of electrostatic interaction and so on. In fact, in order to calculate the thermodynamic radius, R_T, we have used the directly measured A_2^* value

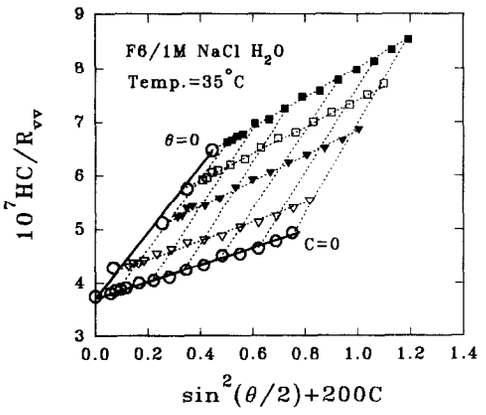

Figure 3 A typical Zimm plot of the F6 fraction in 1 M NaCl mixture solvent

Table 1 Molecular characteristics of branched polyethyleneimine fractions at 35°C

Fraction code	M_w (10^4 g mol^{-1})	M_w/M_n	$[\eta]$ (ml g^{-1})	A_2^* (10^{-4} mol cm^3 g^{-1})	Huggins coefficient
F1	1.66	2.1	10.4		0.77
F2	9.04	1.9	18.9	3.15	0.74
F3	25.8	2.2	25.9	1.75	0.78
F4	44.3	1.8	28.0	1.34	0.77
F5	58.1	2.0	32.3	1.22	0.71
F6	242.	2.2	50.3	0.583	0.77
F7	532.	2.1	64.4	0.316	0.78

Table 2 Radii of branched polyethyleneimine fractions in 1 M NaCl aqueous mixture solvent at 35°C

Fraction code	M_w (10^4 g mol^{-1})	R_G (nm)	R_H (nm)	R_V (nm)	R_T (nm)
F1	1.66		3.2	3.0	
F2	9.04		7.6	6.5	6.3
F3	25.8	16.0	11.7	10.2	10.5
F4	44.3	20.0	13.5	12.5	13.8
F5	58.1	22.5	15.2	14.4	16.0
F6	242.	43.0	33.0	26.8	32.3
F7	532.	57.5	48.0	37.8	44.6

rather than the A_2 value of the pure water solvent system since the use of A_2^* gives a more reasonable R_T value relative to other different radii of the same polymer chain. All the static properties of each fraction such as M_w, R_G and A_2^* are obtained from the Zimm plot, as typically shown in *Figure 3* and are summarized in *Tables 1* and *2*.

Figure 4 shows the variation of the apparent translational diffusion constant D [$= (\langle\Gamma\rangle/q^2)_{\theta=0}$] as a function of polymer concentration. As the concentration dependence of D is very small within the concentration range of this experiment, we do not try to measure the virial coefficient of the diffusion constant, k_d, of equation (9). Instead of the concentration dependence of $\langle\Gamma\rangle/q^2$, we examine thoroughly the angular dependence of $\langle\Gamma\rangle/q^2$ in the dilute regime. In the high q and finite concentration regime, the q and concentration dependence of $\langle\Gamma\rangle/q^2$ can be expressed as[14]:

$$(\langle\Gamma\rangle/q^2) = D_0(1 + f q^2 R_G^2)(1 + k_d C) \qquad (9)$$

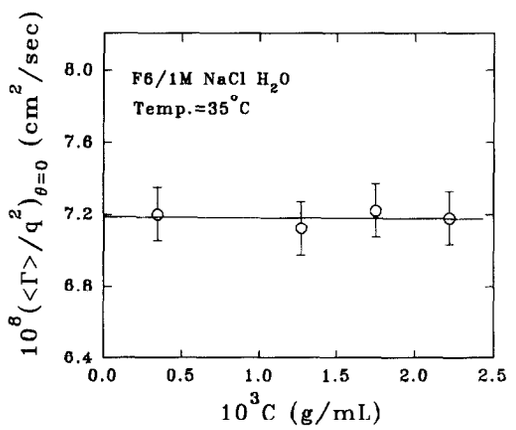

Figure 4 A plot of the apparent translational diffusion constant against concentration

Figure 5 is a plot of the normalized $(\langle\Gamma\rangle/q^2)_{C=0}$ of several fractions *versus* q^2. The low M_w fraction, F4, of small R_G (= 20 nm) shows no angular dependence, whereas the high M_w fraction, F7, has a very steep slope. The f values are calculated from the R_G values and the slopes of *Figure 5*, and plotted as a function of molecular weight in *Figure 6*. There is no molecular weight dependence in the f value (~0.13), which appears small compared with the theoretical f value of 0.2 for a linear polymer with the same polydispersity of $M_w/M_n = 2$ (ref. 14). This result also agrees qualitatively with the theoretical prediction that the f value decreases with branching[14].

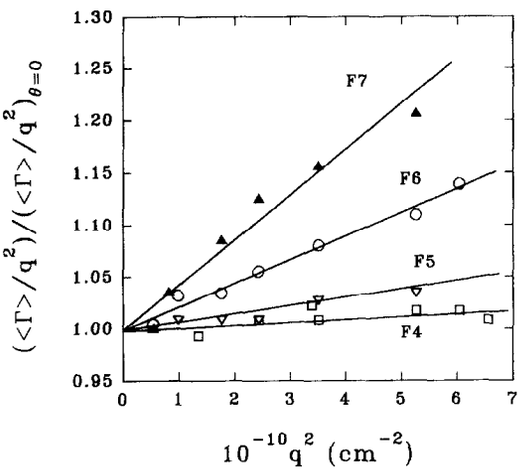

Figure 5 q^2 dependence of the normalized $(\langle\Gamma\rangle/q^2)$ in the dilute concentration regime. The fractions of higher molecular weight show a steep slope

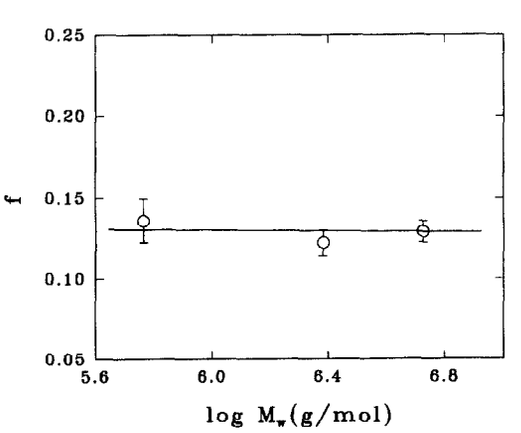

Figure 6 A plot of f factor *versus* molecular weight. The fractions have almost the same f value of ~0.13

Viscosity

The intrinsic viscosity of each fraction, $[\eta]$, and the Huggins coefficient, K_H, measured in the 1 M NaCl aqueous mixture solvent are listed in *Table 1*. It is noticeable that the K_H values of all fractions are large and have the same magnitude of 0.76 ± 0.03. According to Batchelor[23], the Huggins coefficient, K_H, becomes 0.34 for a linear chain in a good solvent and 0.99 for a hard sphere, respectively. Thus, the large K_H values of all fractions indicate that from the rheological point of view, even the low M_w BPEI fraction of $\sim 10^4$ g mol^{-1} has the same structure as the high M_w fraction. Bauer *et al.*[13] reported a similar result; in the multi-armed polyisoprene system, the Huggins coefficient showed a strong dependence mainly on the number of arms, f_{arm}, rather than on the molecular weight (for instance, for the same $f_{arm} = 18$, K_H kept an almost constant value of 0.77 ± 0.02 in the range of M_w from 9.3×10^4 to 3.57×10^6 g mol^{-1}). *Figure 7* shows the log–log plot of the intrinsic viscosity *versus* the weight-average molecular weight. The resulting Mark–Houwink relation, $[\eta] = KM_w^a$ is expressed as:

$$[\eta] = 0.513 M_w^{0.31 \pm 0.01} (\text{ml g}^{-1}, 1.8 \leq M_w/M_n \leq 2.2) \quad (10)$$

As the exponent of the Mark–Houwink relation for the flexible, linear polymer system is about 0.7 in a good solvent and 0.5 in the theta condition, our experimental value of 0.31 is noticeably low. This is ascribed to the very compact structure of BPEI. If the structure of the polymer chain is the perfect hard sphere, the exponent will be 0. Therefore, it still does not reach the hard sphere limit. When compared with the relation ($[\eta] = 0.15 M_w^{0.39}$) reported by Van Den Berg *et al.* in 1973[16], there are some differences in both the exponent, a, and the prefactor, K. Intuitively, the exponent depends mainly on the solvent quality and/or the different degree of branching. In our case, the latter seems to be the main reason since salt-added water was used as the solvent in both experiments and there is no guarantee of the same degree of branching between the two samples used. Next we investigated what caused the large difference between the two measured values of the prefactor. Since, experimentally, the measured intrinsic viscosity of a mixture of monodisperse fractions is a weight-average quantity, the intrinsic viscosity of the polydisperse polymer sample is given as the sum of the intrinsic viscosity of each monodisperse fraction[24], i.e. $[\eta] = \Sigma w_i [\eta]_i$, where $[\eta]_i (= K_0 M_i^a)$ is the intrinsic viscosity of a monodisperse molecular weight M_i fraction and w_i is its weight fraction, respectively. The relation between the prefactor K of the polydisperse samples and the prefactor K_0 of the monodisperse ones may be written as:

$$K = \frac{[\eta]}{M_w^a} = K_0 \left(\frac{\Sigma w_i M_i^a}{(\Sigma w_i M_i)^a} \right) \quad (11)$$

Here we assume that the exponent a of polydisperse samples is same as that of the monodisperse ones as far as the M_w/M_n values of all polydisperse samples are the same. Statistically, for $a < 1$, the right-hand term of equation (11), $\Sigma w_i M_i^a / (\Sigma w_i M_i)^a$ becomes smaller than unity as the *MWD* becomes broader. If the difference between the polydispersity indices of two samples (our samples: $M_w/M_n \cong 2$, and theirs: $M_w/M_n \cong 4$) is taken into account, the difference of the prefactor K can be explained to some extent.

The second virial coefficient

Generally, the second virial coefficient of a linear polymer exhibits a molecular weight dependence with a negative exponent of -0.2 at the good solvent limit. As shown in *Figure 8*, a large negative exponent of -0.53 is obtained. This is further experimental evidence that our BPEI chains have a more compact structure than the linear polymer chains since the molecular weight dependence of the thermodynamic radius scales with the exponent of 0.49 [$= (2 - 0.53)/3$], which is much smaller than the exponent of 0.6 [$= (2 - 0.2)/3$] for the linear chain.

$$A_2^* = 0.135 M_w^{-0.53 \pm 0.02}$$
$$(\text{mol cm}^3\,\text{g}^{-2}, 1.8 \leq M_w/M_n \leq 2.2) \quad (12)$$

Scaling relations of BPEI dimensions

Figure 9 shows the log–log plot of the z-average radius gyration R_G *versus* the molecular weight M_w. The molecular-weight dependence of R_G again appears much lower than the typical Flory's exponent (~ 0.6) of the linear polymer chain at the good solvent limit. This behaviour is also qualitatively consistent with other

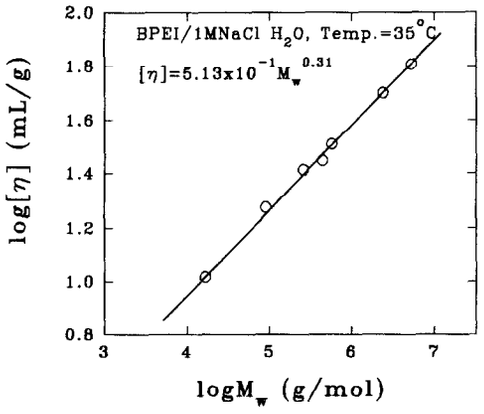

Figure 7 Mark–Houwink plot for branched polyethyleneimine in 1 M NaCl aqueous mixture solvent

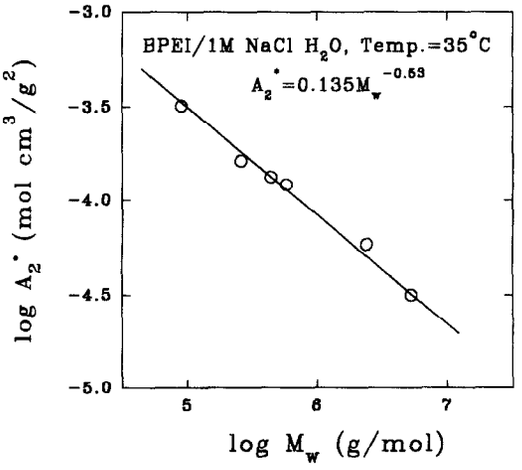

Figure 8 The log–log plot of the second virial coefficient *versus* the weight-average molecular weight

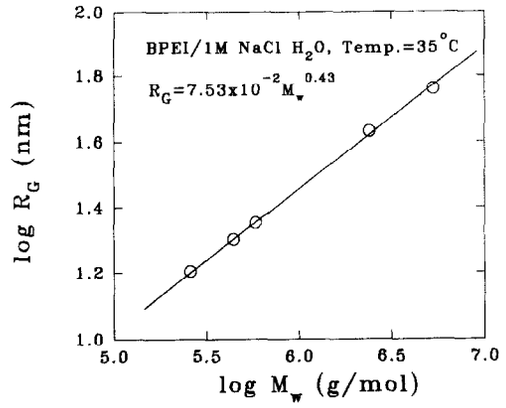

Figure 9 The log–log plot of the z-average radius of gyration, R_G, *versus* the weight-average molecular weight

observations such as the large K_H value, the small f value, the large negative exponent of A_2^* and so on. According to other workers, for a randomly branched polymer, the exponent ν of the R_G on the molecular weight ($R_G \sim M^{\nu}$) is 1/2 in a good solvent and 7/16 in a theta solvent, respectively[25–28]. Although our experimental condition belongs to the good solvent regime, our experimental value of $\nu = 0.43$ appears to be rather close to the theoretical value (0.4375) in the theta condition. This experimental observation may support the proposition that our BPEI samples really have a randomly branched structure. A similar log–log plot of the effective hydrodynamic radius R_H *versus* the molecular weight is shown in *Figure 10*. When the exponent of the molecular weight dependence of R_H is indirectly calculated from the exponent of the Mark–Houwink equation using the simple relation $M[\eta] \sim R_H^3$ [i.e. $0.44 = (1 + 0.31)/3$], there is some difference from the measured value of 0.46. Weill and des Cloizeaux[29], however, reported that the intrinsic viscosity contained both static and hydrodynamic contributions through the relation of $M[\eta] \sim R_G^2 R_H$. This time, the exponent of R_V can be estimated according to the theory of Weill and des Cloizeaux [i.e. $0.44 = (0.43 \times 2 + 0.46)/3$] and it was found that there is good agreement between the calculated value and the experimental value of 0.44. All scaling relations between basic dimensional quantities and molecular weight are summarized as:

$$R_G = 7.53 \times 10^{-2} M_w^{0.43 \pm 0.01} \text{ (nm; } 1.8 \leq M_w/M_n \leq 2.2) \quad (13)$$

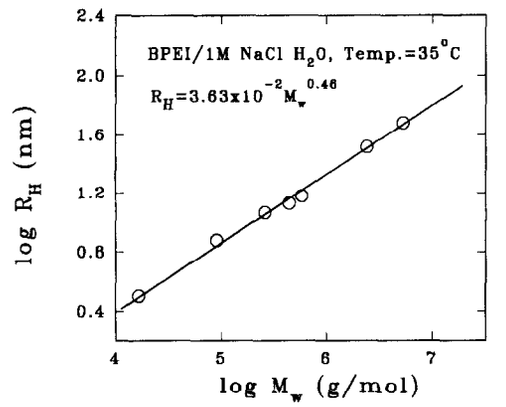

Figure 10 The log–log plot of the z-average hydrodynamic radius, R_H, *versus* the weight-average molecular weight

$$R_H = 3.63 \times 10^{-2} M_w^{0.46 \pm 0.01} \text{ (nm; } 1.8 \leq M_w/M_n \leq 2.2) \quad (14)$$

$$R_V = 4.34 \times 10^{-2} M_w^{0.44 \pm 0.005} \text{ (nm; } 1.8 \leq M_w/M_n \leq 2.2) \quad (15)$$

$$R_T = 2.54 \times 10^{-2} M_w^{0.48 \pm 0.01} \text{ (nm; } 1.8 \leq M_w/M_n \leq 2.2) \quad (16)$$

Size ratio of two different radii

In the monodisperse, linear polymer system, the size ratios of two different radii such as R_G/R_H and R_H/R_V are independent of molecular weight and are well known as the universal ratios[30,31]. In our branched polymer system, as shown in *Figure 11*, all size ratios show molecular weight dependence, in contrast to the linear polymer system. Three different kinds of size ratios are discussed in particular. First of all, (i) R_G/R_H: Recently Oono and Kohmoto[32] predicted 1.24 for the non-draining Gaussian chain limit and 1.562 for the non-draining self-avoid-walk chain in their renormalization group calculation. For linear polymers in a good solvent, many experimental results verify that the R_G/R_H ratio shows M_w independence with a value in the range 1.5–1.7[33]. In *Figure 11*, our experimental value appears to be $\sim$1.55 at the low molecular weight of 10^4 g mol^{-1} and $\sim$1.23 at the high molecular weight of 10^7 g mol^{-1}. If we recall that the ratio is 0.775 at the hard sphere limit[15], we can conclude that the branching effect on this size ratio increases with increasing molecular weight and that the structure of BPEI even at the high molecular weight of 10^7 g mol^{-1} is still far from a hard sphere. (ii) R_G/R_T: In *Figure 11*, it can be seen that this ratio of statically determined radii decreased rapidly with increasing M_w (from 1.75 at 10^4 g mol^{-1} to 1.25 at 10^7 g mol^{-1}). When compared with the theoretical value[15] of 1.41 for a linear polymer in a good solvent and that of 0.775 at the hard sphere, we observed considerably larger values than 1.41 especially in the range of $M_w < 10^6$ g mol^{-1}. Maybe this results from the slightly high index of polydispersity ($M_w/M_n \sim 2$) of our fractions. The broad *MWD* increases the z-average R_G but decreases the R_T due to the negative exponent of $A_2^*(\sim M_w^{-0.54})$. Next, at first inspection, the ratio of R_G/R_T seems to be more sensitive

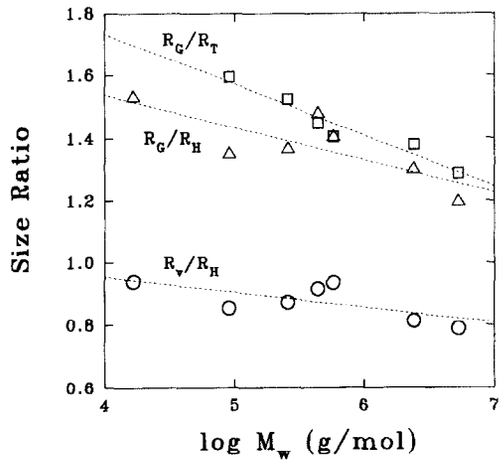

Figure 11 Variation of the calculated size ratios as a function of the molecular weight. The dashed lines are guides to the eyes

to the branching effect than any other size ratio. A similar trend was reported by Bauer *et al.*[13] for the multiarmed polyisoprene, in which R_G/R_T decreased rapidly on increasing the number of arms, f_{arm}, from 1.45 for linear polyisoprene and then levelled off near the hard sphere value, 0.775, at large $f_{arm}(> 30)$. However, Mays *et al.*[30] and Lews *et al.*[31] recently reported that, even in the linear poly(α-methylstyrene)/butyl chloride system, the R_G/R_T showed strong M_w dependence and, in contrast, almost no M_w dependence in the linear polystyrene/2-butanone system. Such a discrepancy might be attributed to the very sensitive character of the thermodynamic radius on the solvent quality. For instance, in a theta solvent, R_T becomes zero while R_G has the ideal dimension. More studies are needed in order to understand clearly the dependence of R_G/R_T on the degree of branching and the molecular weight. (iii) R_V/R_H: For a linear polymer chain, theory predicts that $R_V/R_H = 1.036$ in a non-draining good solvent, 1.075 at the theta condition, and 1.00 at the hard sphere limit[15]. It was also reported that the experimental values of R_V/R_H kept constant in the range of 0.95–1.2 for several branching architectures[12,13] as well as for the linear structure of polystyrene[31,34] and polyisobutylene[35]. However, our experimental data show the weak molecular weight dependence (i.e. from 0.95 to 0.80 for the three-order change in M_w) and lower values compared with the theoretical limiting value of 1.00. First, overall underestimation of R_V/R_H ratio comes again from the slightly high polydispersity index of our BPEI fractions. This is supported by our findings[36] that for the same M_w, the intrinsic viscosity decreases slowly with increasing polydispersity, unlike the z-average quantities such as R_G and R_H. Second, the molecular-weight dependence of R_V/R_H might be due to the scaling property of $R_V \sim R_G^{2/3} R_H^{1/3}$, as mentioned previously. As far as the theory of Weill and des Cloizeaux goes[29], the relative variation of R_V/R_H can reach up to a maximum of 60%* for the conformational change of a linear polymer chain from the non-draining self-avoiding-walk to the hard sphere limit. This appears to be much larger than the Douglas calculation[15] of a maximum of 7.5% [1.075 = 1.075/1.00]. Thus, it will also be interesting to study how R_V/R_H varies in the coil-to-globule transition of the linear polymer chain as well as with the degree of branching.

ACKNOWLEDGEMENTS

The present study was supported by the Korean Science and Engineering Foundation (Grant No. 921-0300-001-2) and the laser light scattering instrument was purchased with the seventh IBRD loan.

REFERENCES

1 Small, P. A. *Adm. Polym. Sci.* 1975, **18**, 1 and references therein
2 Roovers, J. E. L. and Bywater, S. *Macromolecules* 1976, **9**, 873
3 Roovers, J. *Polymer* 1979, **20**, 843
4 Masuda, T., Ohta, Y. and Onogi, S. *Macromolecules* 1986, **19**, 2524
5 Taromi, F. A., Grubisic-Gallot, Z. and Rempp, P. *Eur. Polym. J.* 1989, **25**, 1183
6 Axelson, D. E. and Knapp, W. C. *J. Appl. Polym. Sci.* 1980, **25**, 119
7 Lecacheux, D., Lesec, J. and Quivoron, C. *J. Appl. Polym. Sci.* 1982, **27**, 4867
8 Chu, B., Onclin, M. and Ford, J. R. *J. Phys. Chem.* 1984, **88**, 6566
9 Bugada, D. C. and Rudin, A. *J. Appl. Polym. Sci.* 1987, **33**, 87
10 Pang, S. and Rudin, A. *Am. Chem. Soc., Polym. Mater. Sci. Eng.* 1991, **65**, 95
11 Park, W. C. and Graessley, W. W. *J. Polym. Sci., Polym. Phys. Edn* 1977, **15**, 71
12 Wang, Q. W., Park, I. H. and Chu, B. *Am. Chem. Soc. Symp. Ser.* 1987, **352**, 240
13 Bauer, B. J., Fetters, L. J., Graessley, W. W., Hadjichristidis, N. and Quack, G. F. *Macromolecules* 1989, **22**, 2337
14 Burchard, W. *Adv. Polym. Sci.* 1983, **48**, 1
15 Douglas, J. F., Roovers, J. and Freed, K. F. *Macromolecules* 1990, **23**, 4168
16 Van Den Berg, J. W. A., Bloys van Treslong, C. J. and Polderman, A. *Rec. Trav. Chim.* 1973, **92**, 3
17 Dick, C. R. and Ham, G. E. *J. Macromol. Sci.-Chem.* A 1970, **4**, 1301
18 Mark, H. F. *et al.* (Eds.), 'Encyclopedia of Polymer Science and Technology', 2nd Edn., Vol. 1, John Wiley, New York, 1985, pp. 680–723
19 Huglin, M. B. (Ed.) 'Light Scattering from Polymer Solutions', Academic Press, New York, 1972, Ch. 16
20 Naoki, M., Park, I. H., Wunder, S. L. and Chu, B. *J. Polym. Sci., Polym. Phys. Edn* 1985, **23**, 2567
21 Flory, P. J. 'Principles of Polymer Chemistry', Cornell University Press, Ithaca, NY, 1953
22 Yamakawa, H. 'Modern Theory of Polymer Solutions', Harper and Row, New York, 1971
23 Batchelor, G. K. *J. Fluid Mech.* 1977, **83**, 97
24 Rosen, S. L. 'Fundamental Principles of Polymeric Materials', Wiley, New York, 1992, Ch. 6
25 Patton, E. V., Wesson, J. A., Rubinstein, M., Wilson, J. C. and Oppenheimer, L. E. *Macromolecules* 1989, **22**, 1946
26 Isaacson, J. and Lubensky, T. C. *J. Phys. Lett. (Paris)* 1980, **41**, L469
27 Daoud, M. and Joanny, J. F. *J. Phys. (Paris)* 1981, **42**, 1359
28 Daoud, M., Family, F. and Jannink, J. *J. Phys. Lett. (Paris)* 1984, **45**, L199
29 Weill, G. and des Cloizeaux *J. Phys. (Paris)* 1979, **40**, 99
30 Mays, J. W., Nan, S. and Lewis, M. *Macromolecules* 1991, **24**, 4857
31 Lews, M. E., Nan, S., Yunan, W., Li, J. and Mays, J. W. *Macromolecules* 1991, **24**, 6686
32 Oono, Y. and Kohmoto, M. *J. Chem. Phys.* 1983, **78**, 520
33 Park, S., Chang, T. and Park, I. H. *Macromolecules* 1991, **24**, 5729
34 Fetters, L. J., Hadjichristidis, N., Lindner, J. S., Mays, J. W. and Wilson, W. W. *Macromolecules* 1991, **24**, 3127
35 Lewis, M. E., Nan, S. and Mays, J. W. *Macromolecules* 1991, **24**, 197
36 Park, I. H. and Kim, J. H. *J. Adv. Mater. (KNUT)* 1994, **1**, 1
37 Roovers, J. and Toporowski, P. M. *J. Polym. Sci., Polym. Phys. Edn* 1980, **18**, 1907
38 King, T. A., Knox, A. and McAdam, J. D. G. *Polymer* 1973, **14**, 293

* If $R_V \sim R_G^{2/3} R_H^{1/3}$, R_V/R_H scales as $(R_G/R_H)^{2/3}$. In this particular case, $(R_V/R_H)_{saw}/(R_V/R_H)_{hs} \sim \{(R_G/R_H)_{saw}/(R_G/R_H)_{hs}\}^{2/3} = (1.562/0.775)^{2/3} = 1.60$, where the subscripts saw and hs indicate self-avoiding-walk and hard sphere, respectively